

NO-A193 461

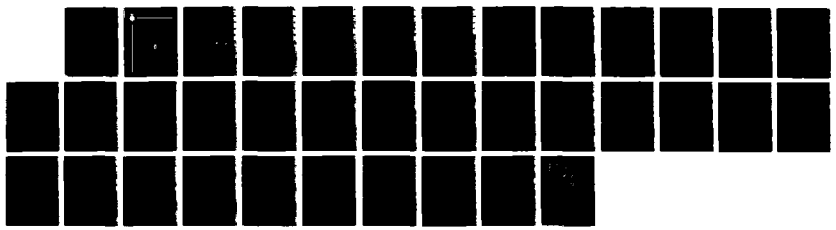
SHEAR STRESS AT A FILM-SUBSTRATE INTERFACE DUE TO
MISMATCH STRAIN(U) BROWN UNIV PROVIDENCE RI DIV OF
ENGINEERING L B FREUND ET AL. JAN 88 N00014-87-K-0481

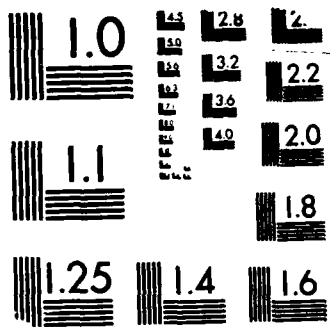
1/1

UNCLASSIFIED

F/G 20/12

NL





MICROCOPY RESOLUTION TEST CHART
NBS 1963-A



Brown University
DIVISION OF ENGINEERING
PROVIDENCE, R.I. 02912



AD-A193 461

DTIC FILE COPY

Shear Stress at a Film-Substrate Interface
Due to Mismatch Strain

by

L. B. Freund and Y. Hu
Division of Engineering
Brown University
Providence, RI 02912

DTIC
ELECTE

DTIC
ELECTE
MAR 30 1988
S D

DISTRIBUTION STATEMENT A
Approved for public release
Distribution Unlimited

88 2 25 010

1

*D. Lee Kuchner
11325A*

Shear Stress at a Film-Substrate Interface
Due to Mismatch Strain

by

L. B. Freund and Y. Hu
Division of Engineering
Brown University
Providence, RI 02912

DTIC
SELECTED
MAR 30 1988
S D D

DISTRIBUTION STATEMENT A
Approved for public release
Distribution Unlimited

Office of Naval Research
Contract N00014-87-K-0481

IBM Corporation
Research Award in Materials Science

January 1988

SHEAR STRESS AT A FILM-SUBSTRATE INTERFACE

DUE TO A MISMATCH STRAIN

L. B. Freund and Y. Hu
Laboratory for Interface Science and Engineering
and
Division of Engineering
Brown University
Providence, RI 02912

ABSTRACT

The elastic stress distributions that develop when a thin film of one material is bonded to a half space of a second material under conditions with a mismatch strain that results in a state of residual stress. The origin of the mismatch strain may be temperature change, chemical reaction, remote applied loading on the substrate, or some other source. The distribution of shear stress at the interface is determined for the case when the film is thin enough to be idealized as a membrane. A semi-infinite film is considered first to examine in detail the concentration of shear stress near the edge. Then, a periodic array of film segments is considered, and the dependence of the stress distribution and the stress concentration factor on spacing and material parameters is determined. The special case of an isolated film segment is studied by taking the spacing distance to be very large compared to the segment width. All problems are cast in the form of a singular integral equation for the distribution of shear stress at the interface, and this integral equation is solved numerically for the cases of interest. Representative results are also presented for the distribution of mean stress and resolved shear stress in the substrate due to the mismatch strain. Finally, the limitations of the film idealization of the substrate are discussed.



Accession For	
NTIS CRA&I	<input checked="" type="checkbox"/>
DTIC TAB	<input type="checkbox"/>
Unannounced	<input type="checkbox"/>
Justification	
By <i>per ltr</i>	
Distribution/	
Availability Codes	
Dist	Avail and/or Special
<i>A1</i>	

1. INTRODUCTION

During fabrication of bi-material systems, mechanical strains that are incompatible with a stress-free state are often introduced unintentionally. These strains may arise from thermal processing, reaction swelling or shrinking, alloying or other fabrication procedure. The joining of the materials across a common interface enforces a kinematic compatibility that may result in a distribution of mechanical stress throughout the materials. If conditions are not too severe, the stress is elastic over most of the region of the bodies.

As the most elementary example of this phenomenon, consider a thin film bonded to a relatively massive substrate. Any edge effects are ignored for the moment, so the film is taken to be of unbounded extent in the plane of the common interface and the substrate is assumed to be a half space. Suppose that the coefficients of linear thermal expansion of the film and substrate are α and α_s , respectively. If the entire system then undergoes a temperature change ΔT , an isotropic membrane tensile stress

$$\sigma_o = \frac{E}{1 - \nu} \Delta T (\alpha_s - \alpha) \quad (1.1)$$

is induced in the film. It is tacitly assumed in writing (1.1) that, because of the bulk of the substrate compared to the film, the substrate expands freely and it merely imposes its extensional strain on the layer in all directions parallel to the common interface plane.

At this level of analysis, the interaction of the film and the substrate is completely overlooked. Load is transferred from the layer to the substrate in an unspecified way at remote points and, in the region where the film carries the stress (1), the interface is traction free. This is at variance with the common belief that the differential strain provides the mechanical driving force for film-substrate separation or other mechanical failure mode. For such separation to occur, there must some traction acting on the interface. This traction arises from the transfer of load from the substrate to the film and it is typically concentrated near the edge of the film. In the next section, a simple

analytical model is developed that leads to an estimate of interface stress near the edge of a thin bonded layer in the presence of a differential strain.

The mechanical stress concentration near the edge of the film can lead to some undesirable mechanical consequences. For example, the stress may be large enough to produce a separation or fracture of the interface, or it may relax by forcing crystal dislocations into the substrate material from the edge. Of equal interest in other related work underway, however, is the influence of this stress distribution on nonmechanical phenomena that are of concern in fabrication and performance of microelectronic and micro-optical devices. For example, the edge stress field may influence the electrical properties of the configuration in the case when the substrate material is piezoelectric. This issue is relevant to the case of a field effect transistor (FET), for instance, for which the substrate material is gallium arsenide and the gate material is tungsten silicide or some other suitable conducting material. The influence of the residual stress distribution on the threshold voltage of a FET due to the piezoelectric effect has been studied by Ramirez et al (1987). The presence of this edge stress field can also lead to anomalous diffusion of a dopant or other second species, particularly in the presence of material defects near the film edge.

The present analysis is aimed at understanding the effect of certain geometrical features on the interfacial stress distribution due to a differential strain between the film and substrate. First, the traction distribution on the interface between a semi-infinite thin film and a substrate is determined. This result gives a clear picture of the asymptotic properties of the interfacial traction distribution, which are also considered on the basis of a conservation integral of elasticity. The problem of induced stress in a substrate due to a semi-infinite film was studied in a similar way by Hu (1979). Next, the case of a periodic array of films is analyzed. The case of a single film of finite extent emerges as a special case when the periodic gap between films is very large, and other special cases may be considered as well. Finally, the range of validity of this model is considered by examining the pertinent elasticity solutions for points very close to the edge and very far from the edge compared to the film thickness. With this stress

distribution in hand, the complete stress field within the substrate may be determined.

2. THE INTERFACIAL SHEAR STRESS NEAR AN EDGE

The two dimensional geometry of the system used to examine the edge stress is shown in Fig. 1a. In effect, the film and substrate are initially stress and deformation free. Then, an extensional strain ϵ_o , *isotropic in the plane of the interface*, is imposed on the film and the film is bonded to the substrate. To enforce this strain, of course, a stress

$$\sigma_o = \frac{E}{1 - \nu} \epsilon_o \quad (2.1)$$

must be imposed on the film edge. After the film is bonded to the substrate, the stress on the edge is relaxed. The film now has a traction free edge at $x = 0$, and therefore it cannot support the uniform all-around tensile stress (2.1). Instead, the tensile stress in the x -direction in the film must vary from zero at $x = 0$ to the value given in (2.1) at values of x many time greater than the film thickness h . This variation in tensile stress in the film must be accompanied by a shear traction at the film-substrate interface which also varies with x , and a main purpose in this section is to determine this shear traction distribution. To this end, the extensional strains in the x -direction of both the film and the substrate surface $z = 0$ are written in terms of the unknown interface shear stress $\tau(x)$. Imposition of the physical requirement that these two extensional strains are equal leads to an integral equation for $\tau(x)$.

In the inset in Fig. 1b, the film and substrate are shown to be separated but to be under action of equal but opposite internal shear traction. The film is considered first. If the tensile stress acting on a cross section at distance x from the free end is $\sigma(x)$, then the overall equilibrium of the film requires that

$$h\sigma(x) = \int_0^x \tau(x') dx' . \quad (2.2)$$

The stress-strain relation for the film (modelled as a membrane) that properly accounts for a mismatch strain of ϵ_o is

$$\epsilon_f(x) = \frac{1 - \nu^2}{E} \sigma(x) - \epsilon_o(1 + \nu) \quad (2.3)$$

where $\epsilon_f(x)$ and ϵ_o are the relaxation strain in the x -direction and differential strain, respectively, in the film. Note that if $\epsilon_f \rightarrow 0$ at points far from the edge, then according to (2.3) the stress σ approaches the tensile stress σ_o in (2.1), that is, equations (2.1) and (2.3) are consistent. The result of eliminating $\sigma(x)$ from between (2.2) and (2.3) is

$$\epsilon_f(x) = \frac{1 - \nu^2}{E} \int_0^x \tau(x') dx' - \epsilon_o(1 + \nu). \quad (2.4)$$

A result similar to (2.4) for the substrate is next derived. For plane strain, the relation between the extensional strain in the x -direction $\epsilon_x(x)$ and the corresponding stress component $\sigma_x(x)$ is

$$\epsilon_{xx}(x) = \frac{1 - \nu_s^2}{E_s} \sigma_{xx}(x). \quad (2.5)$$

This equation applies at any point of the substrate but, in particular, on the surface $z = 0$. From the theory of elasticity (Timoshenko and Goodier, 1970), the stress σ_{xx} along $z = 0$ due to a concentrated force acting at $x = x'$ of magnitude $P(x')$ is $-2P(x')/\pi(x - x')$. Thus, replacing $P(x')$ by $\tau(x') dx'$ and summing over the entire range of $\tau(x')$,

$$\epsilon_{xx}(x) = -\frac{2(1 - \nu_s^2)}{\pi E_s} \int_0^\infty \frac{\tau(x') dx'}{x - x'}. \quad (2.6)$$

Because the film and substrate are bonded together as the strains ϵ_f and ϵ_{xx} develop, these two strains must be equal. Thus,

$$\frac{(1 - \nu^2)}{Eh} \int_0^x \tau(x') dx' + \frac{2(1 - \nu_s^2)}{\pi E_s} \int_0^\infty \frac{\tau(x') dx'}{x - x'} - (1 + \nu)\epsilon_o = 0 \quad (2.7)$$

for $0 < x < \infty$. This is a linear integral equation for the unknown shear traction $\tau(x)$. The shear traction is proportional to ϵ_o , which may be positive or negative. The solution of (2.7) is considered next.

The integro-differential equation (2.7) has the form of Prandtl's equation for the aerodynamic load distribution over a wing of finite span in a steady air flow (Muskhelishvili, 1953). The same equation has been studied by Koiter (1955) in the context of structural mechanics, where he was concerned with load transfer characteristics in

stiffened elastic sheets. Koiter obtained a formal solution of this equation in the form of an infinite series by means of integral transform methods and analytic function theory. Explicit limiting results that are useful for dealing with the problem at hand may be extracted from Koiter's work, and the details of his solution procedure are not reproduced.

Nondimensional coordinates are introduced as $\xi = \kappa x/h$ and $\xi' = \kappa x'/h$ in terms of a dimensionless material parameter $\kappa = E_s(1 - \nu^2)/E(1 - \nu_s^2)$. The equation (2.7) governing the normalized shear stress $f(\xi) = \tau(x)/\kappa\sigma_0$ becomes

$$\int_0^\xi f(\xi') d\xi' - \frac{2}{\pi} \int_0^\infty \frac{f(\xi')}{\xi' - \xi} d\xi' - 1 = 0 \quad (2.8)$$

for $0 < \xi < \infty$. An auxiliary condition on the solution of (2.8) concerning the behavior of $f(\xi)$ as $\xi \rightarrow \infty$ is obtained from (2.2). If it is recalled that $\epsilon_f(x) \rightarrow 0$ as $x \rightarrow \infty$, then the dimensionless form of the limiting equation is

$$\int_0^\infty f(\xi') d\xi' = 1. \quad (2.9)$$

Thus, a solution of (2.8) subject to (2.9) is required.

The Mellin transform defined by

$$F(s) = \int_0^\infty f(\xi) \xi^{s-1} d\xi \quad (2.10)$$

is applied to (2.8) and (2.9), and the determination of $f(\xi)$ is thereby reduced to the solution of the difference equation

$$F(s+1) = -2s \cot(\pi s) F(s) \quad (2.11)$$

subject to the auxiliary condition $F(1) = 1$. Koiter (1955) presented the solution of (2.11) in the form

$$F(s) = \frac{2^{s-1} G(s+1)G(5/2-s)}{\sqrt{\pi} G(s-1/2)G(2-s)} \quad (2.12)$$

where the function $G()$ is defined as

$$G(s + 1) = (2\pi)^{s/2} e^{-\frac{1}{2}s(s+1) - \frac{1}{2}\gamma s^2} \prod_{n=1}^{\infty} \left\{ (1 + s/n) e^{-s + s^2/2n} \right\} \quad (2.13)$$

and $\gamma = 0.57722$ is Euler's constant. The dimensionless shear stress itself is then given by the Mellin transform inversion integral

$$f(\xi) = \frac{1}{2\pi i} \int_{b-i\infty}^{b+i\infty} F(s) \xi^{-s} ds \quad (2.14)$$

where $1/2 < b < 1$. For $\xi > 0$, the integration path in (2.14) may be closed by a semicircle of very large radius in the left half of the complex s -plane without affecting the value of the integral. The function $F(s)$ has discrete n -tuple poles at $s = 3/2 - n$, $n = 1, 2, 3, \dots$ in the left half plane and no other singularities there, so that application of Cauchy's integral formula yields the result that the value of $f(\xi)$ is the sum of the residues of these poles, that is,

$$f(\xi) = \sum_{n=1}^{\infty} [\text{residue of } F(s) \xi^{-s} \text{ at } s = 3/2 - n]. \quad (2.15)$$

Some details are given by Koiter (1955).

For small values of ξ , that is, for points close to the free end of the film, the behavior of $f(\xi)$ is dominated by the first few terms in (2.15). Evaluation of the first two terms yields

$$f(\xi) \approx (2\pi\xi)^{-1/2} - 0.21938 \xi^{1/2} + 0.12698 \xi^{1/2} \ln \xi \quad (2.16)$$

which is a good approximation for $0 < \xi < 2$. For large values of ξ the convergence of the series (2.15) is slow. However, an approximation to $f(\xi)$ for large ξ can be obtained by closing the path of integration in (2.14) in the remote right half plane and evaluating the dominant residues of the enclosed poles. The first two terms of the resulting asymptotic approximation are

$$f(\xi) \approx \frac{2}{\pi \xi^2} - \frac{4}{\pi^2 \xi^3} (1.2319 - 2.0 \ln \xi) \quad (2.17)$$

which is a good approximation for $\xi > 5$. The transition between the asymptotic solutions (2.16) and (2.17) is expected to be smooth.

The dependence of shear stress $\tau(x)$ at the film-substrate interface on position x along the interface is shown in the dimensionless form $\tau(x)/\kappa\sigma_o$ versus $\kappa x/h$ in Fig. 2, where $\kappa = (1 - \nu^2)E_s/(1 - \nu_s^2)E$ and σ_o is related to the mismatch strain through (2.1). The asymptotic approximations for small and large values of $\kappa x/h$ given in (2.16) and (2.17) are shown as dashed lines in Fig. 2. The solid curve is the result of solving the integral equation (2.8) numerically by means of the numerical methods introduced by Erdogan, Gupta and Cook (1973), based on Chebyshev polynomial representation of the unknown function and Gaussian integration. The numerical results are similar to those of Hu (1979) who obtained a solution by a direct finite difference method. It is clear that the numerical solution is consistent with the asymptotic approximations at either end of the range of $\kappa x/h$, and that it provides a smooth transition between the asymptotic approximations. Representative values of κ for several material systems in the form $\kappa(\text{film material}/\text{substrate material})$ are given by $\kappa(Ni/Glass) \approx 2$, $\kappa(Al/GaAs) \approx 4/5$, $\kappa(Au/GaAs) \approx 1/2$ and $\kappa(Au/Si) \approx 1/3$.

Some general observations can be made concerning the stress distribution. The shear stress near the end $x = 0$ is of main interest, and the first term of the asymptotic approximation (2.16) may be written in dimensional form as

$$\tau(x) = \frac{\epsilon_o E}{(1 - \nu)} \sqrt{\frac{h\kappa}{2\pi x}} \quad (2.18)$$

First, it is noted that the shear stress varies linearly with the mismatch strain ϵ_o which is an obvious consequence of linearity of the system. It is also evident from (2.18) that $\tau(x)$ is proportional to $\sqrt{E_s E}$. Thus, a reduction of stiffness of either material component results in a reduction of the stress concentration, other things being fixed. Also, for fixed elastic moduli and mismatch strain, $\tau(x)$ is proportional to \sqrt{h} for any x . Thus, the thickness sets the rate of decay of shear stress from the edge.

The infinite singularity in stress $\tau(x)$ as $x \rightarrow 0$ is unrealistic, of course, in the

sense that no real material can support such a stress. The stress singularity is a consequence of the tacit assumption that the material remains elastic at all stress levels. In reality, the potentially large stress would be relieved locally by some nonlinear relaxation mechanism, but the shear stress would still be concentrated near the edge of the layer. From dimensional considerations, the size of the region over which yielding is expected will scale with the parameter $h\kappa(\sigma_o/\sigma_y)^2$ where σ_y is the tensile yield stress of the material. Finally, it is noted that the asymptotic result (2.18) can be derived directly, without the need to solve the integral equation (2.8), by means of energy methods developed in fracture mechanics. In particular, application of Rice's path independent J-integral (Rice, 1968) leads to the result immediately. When evaluated for any closed path in a body under plane strain conditions that does not enclose body forces or holes, the value of this integral is zero, that is,

$$J(C) = \int_C [Wn_x - \sigma_{ij}n_j u_{i,x}] dC = 0 \quad (2.19)$$

where W is the elastic strain energy density, n_i is the unit vector normal to C , σ_{ij} are the rectangular components of the stress tensor, and u_i are the rectangular components of the displacement vector. Consider the integral in (2.19) for the path C shown in Fig. 3. The radii of the small and large circular arcs in C are assumed to be indefinitely small and large, respectively. The integrand of (2.19) vanishes on all parts of C except on the circular arc AB in the substrate and on the line segment DE in the film. Along the latter segment, it is readily shown that

$$J(DE) = -\frac{(1+\nu)Eh\epsilon_o^2}{2(1-\nu)}. \quad (2.20)$$

The only way for the value of $J(AB)$ to balance this contribution is for the stress to be square root singular in the substrate near the film edge, say

$$\tau(x) = \begin{cases} 0 & \text{for } x < 0 \\ k/\sqrt{2\pi x} & \text{for } x > 0 \end{cases} \quad (2.21)$$

where k is the so-called elastic stress intensity factor of linear elastic fracture mechanics.

If this is the case, then

$$J(AB) = \frac{1 - \nu^2}{2E_s} k^2. \quad (2.22)$$

From the condition that $J(C) = J(AB) + J(DE) = 0$, it follows that $k = \sigma_o \sqrt{h\kappa}$ which reproduces (2.18). The complete stress distribution shown in Fig. 2 can be determined, however, only by solution of the integral equation (2.8).

3. INTERFACIAL SHEAR STRESS FOR A PERIODIC ARRAY OF FILMS

The integral equation (2.8) for interfacial shear stress $\tau(x)$ was generated for the case of a semi-infinite film on a substrate. While this situation provides useful results on the edge effect for very wide films, it provides no basis for assessing the influence of lateral dimension of the film on the stress distribution. The integral equation is readily generalized for the case of films of finite lateral extent or multiple films for this purpose, as illustrated by Yang and Freund (1984). The particular case of a periodic array of films is considered here.

The two dimensional configuration is shown in Fig. 4. Each film has width $2b$ and the separation distance between adjacent films is $2a$. By following the development in section 2, it can be shown that the interfacial shear stress for the film occupying the interval $-b < x < b$ on the substrate surface must satisfy

$$\frac{(1-\nu^2)}{E} \int_{-b}^x \tau(x') dx' + \frac{2(1-\nu^2)}{\pi E_s} \sum_{m=-\infty}^{\infty} \int_{-b+2m(a+b)}^{b+2m(a+b)} \frac{\tau(x')}{x-x'} dx' - (1+\nu)\epsilon_o = 0 \quad (3.1)$$

for $-b < x < b$. The complete elastic field must be periodic in the x -direction with period $2(a+b)$. Consequently,

$$\tau(x) = \tau[x - 2m(a+b)], \quad m = \dots -2, -1, 0, 1, 2, \dots \quad (3.2)$$

In view of this periodicity, the infinite sum in the integral equation may be rewritten as

$$\sum_{m=-\infty}^{\infty} \int_{-b+2m(a+b)}^{b+2m(a+b)} \frac{\tau[x' - 2m(a+b)]}{x-x'} dx' \quad (3.3)$$

With a change of variable of integration in each integral from x' to ξ according to $\xi = x' - 2m(a+b)$, the limits of integration become independent of m , and the order

of summation and integration may be reversed, that is,

$$\sum_{m=-\infty}^{\infty} \int_{-b}^b \frac{\tau(\xi)}{x - \xi - 2m(a+b)} d\xi = \int_{-b}^b \frac{\tau(\xi)}{x - \xi} d\xi + \int_{-b}^b \tau(\xi) \sum_{m=1}^{\infty} \frac{2(x - \xi)}{(x - \xi)^2 - 4m^2(a+b)^2} d\xi. \quad (3.4)$$

The series has a sum in terms of elementary functions given by Gradshteyn and Ryzhik (1965) as

$$\sum_{m=1}^{\infty} \frac{2\theta}{m^2\pi^2 - \theta^2} = \theta^{-1} - \cot \theta \quad (3.5)$$

for the appropriate range of θ . The integral equation is reduced to

$$\frac{(1 - \nu^2)}{Eh} \int_{-b}^x \tau(\xi) d\xi + \frac{(1 - \nu_s^2)}{E_s(a+b)} \int_{-b}^b \tau(\xi) \cot \left[\frac{\pi(x - \xi)}{2(a+b)} \right] d\xi = (1 + \nu)\epsilon_o \quad (3.6)$$

for $-b < x < b$. Note that the cotangent function in the kernel of the integral equation behaves as $2(a+b)/\pi(x - \xi)$ for $(x - \xi) \ll (a+b)$, so that the kernel is still a Cauchy kernel.

The condition that the tension in the film is zero at $x = -b$ is incorporated into (3.6). The tension must also vanish at $x = b$ and, on the basis of overall equilibrium, this will be assured if

$$\int_{-b}^b \tau(\xi) d\xi = 0. \quad (3.7)$$

Thus, a solution of the integral equation (3.6) subject to the auxiliary condition (3.7) is sought.

The numerical method employed in the preceding section once again provides an efficient means of obtaining accurate solutions. Some results on the complete interfacial shear stress distribution are summarized in the form of plots of $\tau(x)/\kappa\sigma_o$ versus $(1+x/b)$ for $-b < x < 0$ in Figs.4 and 5. The results in these variables may be expressed in terms of the two dimensionless parameters $\kappa b/h$ and a/b . The shear stress distribution for several values of $\kappa b/h$ are shown in Fig. 5 for the situation of a single film segment

of width $2b$ on the surface. This is equivalent to the case of periodic films when the individual film segments are widely spaced, that is, when $a/b \rightarrow \infty$ with b/h held fixed. Calculations were carried out for the case of periodic films with $a/b = 20$, and the results were indistinguishable from those in Fig. 5. Likewise, the value $a/b = 1/20$ represents the situation of films with edges in close proximity compared to the lateral extent of each film. The integral equation for two semi-infinite films separated by a gap of $2a$ may be obtained from (3.6) by letting $a/b \rightarrow 0$ with a/h held fixed. This result was also solved independently with the results differing only slightly from those for $a/b = 1/20$.

Shear stress distributions for several combinations of $\kappa b/h$ and a/b are shown in Fig. 6. This figure shows typical results for the influence of film proximity in the periodic array on stress level. Evidently, for a given value of $\kappa b/h$, the level of shear stress is elevated by moving the films closer together, but the overall increase is not significant unless a/b becomes small compared to unity, except possibly for the value of the edge singularity.

The strength of the singularity in interfacial shear stress is defined by

$$k = \lim_{x \rightarrow -b^-} \tau(x) \sqrt{2\pi(x+b)}. \quad (3.8)$$

The influence of geometrical parameters on the edge singularity is shown in Fig. 7. This figure shows plots of the normalized stress intensity factor defined in (3.8) at the edge $x = -b$. From the figure, it is clear that if the film is indeed thin so that $\kappa b/h \ll 1$ and if the individual segments are widely spaced, so that $a/b \geq 1$, then the stress intensity factor is virtually independent of these geometrical parameters. However, for situations other than widely spaced, very thin segments, the figure suggests rather complicated behavior. For example, the dependence of $k/\sigma_o \sqrt{\kappa h}$ on $\kappa b/h$ is fundamentally different for the cases when $a/b > 1$ and $a/b < 1$. Furthermore, for a given value of $\kappa b/h$, the stress intensity factor $k/\sigma_o \sqrt{\kappa h}$ depends strongly on a/b as a/b decreases to values less than unity. Indeed, $k/\sigma_o \sqrt{\kappa h} \rightarrow 0$ as $a/b \rightarrow 0$ for any given value of $\kappa b/h$.

These results have implications for the failure of a very wide single film due to tensile cracking through the thickness, followed by delamination fracture due to the resulting edge stress concentration in the newly created segments. For example, suppose that through the thickness cracks are introduced at widely separated places, say at intervals of $30 h/\kappa$. Then, with reference to Fig. 7, this starting situation corresponds to a point with $\kappa b/h = 15$ and a/b very small, say about $a/b = 0.05$. Further, suppose that the corresponding level of stress intensity factor is large enough to drive delamination fractures in either direction along the interface away from the through-thickness cracks. The effect is to increase the value of the geometrical parameter a/b and to reduce $\kappa b/h$ which, in turn, leads to a reduction in level of stress intensity. Thus, the growth can continue until the value of k has been reduced to a level below that required to sustain growth of delamination cracks, and the process can then stop. For the thin film idealization used here, the portion of the film that is detached from the substrate plays no role whatsoever in determining the stress distribution in the attached portion of the film or in the substrate. Consequently, partially debonded films are treated in the same way as bonded segments with the debonded portion simply ignored.

4. STRESS STATE IN THE SUBSTRATE

Once the interfacial shear stress between the film and substrate is determined the state of stress in the substrate may be calculated by superposition over the appropriate concentrated boundary force solution. For example, an expression for one component of stress is

$$\sigma_{xz}(x, y) = -\frac{2}{\pi} \int_L \frac{\tau(x') dx'}{\sqrt{(x-x')^2 + z^2}} \quad (4.1)$$

where L is the union of intervals in x' along the surface of the substrate that are covered by film segments.

The stress distribution in the substrate has been determined for several combinations of geometrical parameters by numerical evaluation of the integrals such as the one in (4.1). Representative results are shown in Figs. 8 and 9. In Fig. 8, the distribution of mean normal stress in the substrate is shown for the case of periodic film segments with $\kappa b/h = 10$ and $a/b = 0.5$. The result is in the form of a surface over the x, z -plane where the elevation of the surface represents the level of normal stress. A film, which carries residual tension, occupies $-10 \leq \kappa x/h \leq 10$ on $\kappa z/h = 0$, and a gap between identical film segments occupies $10 \leq \kappa x/h \leq 20$. Because of symmetry, results are shown for only half of the film segment and half of the gap, to a depth of $\kappa z/h = 15$ in the substrate. Mean normal stress is selected for presentation because the gradient of this field is the driving force for chemical diffusion of point defects in the substrate. For example, interstitial components in the substrate will diffuse from regions of low mean normal stress to regions of high mean normal stress with transport flux in the direction of the gradient spatial gradient vector. Thus, a qualitative observation based on Fig. 8 is that interstitial components in the substrate will tend to diffuse from under the film into the region under the gap, with maximum concentration developing near the film edge and near the substrate surface in the gap region.

The similar surface in Fig. 9 shown the distribution of resolved shear stress on plane in the substrate inclined at angles of $\pm\pi/4$ to the substrate surface. This stress measure is selected for presentation because of the importance of the resolved shear

stress on dislocation glide planes in a crystalline substrate for dislocation defect generation and motion. The values of the various geometrical parameters are the same for this illustration as for Fig. 8. It is evident that the local interfacial shear stress concentration can be relieved by forcing glide dislocations into the substrate as shown schematically in Fig. 10 and the resolved shear stress shown in Fig. 9 provides the driving force for this process. Figs. 8 and 9 provide some motivation for further study of both the diffusion and dislocation generation issues in connection with the thin film edge stress concentration.

5. ASYMPTOTIC PROPERTIES OF STRESS DISTRIBUTION

The idealization of the film as an elastic membrane in the present study leads to a boundary value problem that is relatively simple. Consequently, the problem can be analyzed in some detail and the results are instructive in illustrating edge stress concentration effects in thin film configurations, at least in a qualitative sense. However, the idealization is quite extreme for certain purposes, and the shortcomings must be kept in mind in considering specific applications.

Essentially, the membrane idealization implies that the film resists deformation only if that deformation includes extension or contraction of the mid-plane of the film. There is no resistance to bending or to transverse shear of the film. While these features are expected to provide a basis for accurate description of the deformation of the film over most of its length, they become suspect at points close to film edges where stress gradients are large (that is, stress changes significantly over distances comparable to film thickness) and where shear deformation effects become important. Because deformation by shear is precluded in the membrane idealization, the response to the edge shear stress observed in the analysis is stiffer than it would be if shear deformation were included. Consequently, the edge stress concentration is more severe than it would be in a more complete description of the edge effect.

Indeed, for points very close to the corner at $x = 0$, $z = 0$ the structure of the mechanical fields may be determined by examining the states of stress that can exist in the case of plane strain deformation of an elastic quarter plane bonded to an elastic half plane. For correspondence to the problem class under study here, the quarter plane should be subject to an extensional mis-match strain of magnitude ϵ_0 in the plane of the common interface. This problem may be treated by the eigen-value approach developed by Bogy (1971) for problems of this type. In particular, it can be shown that the stress field in the vicinity of the corner (that is, within the region where $\kappa r/h \ll 1$ in the present case) varies with distance r from the edge as $r^{-\alpha}$ where α is a root of a transcendental equation in the range $0 < \Re(\alpha) < 0.5$. For the particular case when

the two materials are the same, $\kappa = 1$ and $\alpha = 0.4555$ (Bogy (1971)). In any case, the singularity in stress at the corner is weaker than the membrane model suggests. The membrane model can be expected to provide a good description of the stress fields, taking into account the finite thickness of the layer in some way, only for $\kappa r/h$ greater than about $1/2$.

The stress distribution in the substrate at points far from the film edge compared to the thickness of the film is easy to determine. In all cases in which the film is moderately thin, the interfacial shear stress is concentrated within about one or two film thicknesses of the film edge. Thus for remote points it appears that concentrated forces act at the film edges, and the magnitude of the concentrated force in each case is simply the resultant of the edge stress concentration. For example, in the simplest case of a semi-infinite film discussed in section 2, the resultant force of the interfacial stress distribution is $h\sigma_0$, so the stress distribution in the substrate at points far from the edge compared to the film thickness is that of a concentrated force of this magnitude.

The study of this issue of the edge stress concentration is continuing. In situations where it is important to have accurate quantitative descriptions of stress distributions, it is possible to obtain them by computational methods. This has been done, for example, in a calculation aimed at estimating the influence of the piezoelectric effect on threshold voltage in a field effect transistor. However, the development of simple models of thin film structures is proceeding in parallel in the hope that the general, qualitative results that follow from such models can provide a general framework for the problem area.

Acknowledgments

The research support of the Office of Naval Research through Contract N00014-87-K-0481 and of the IBM Corporation through a Research Award in Materials Science is gratefully acknowledged. We are also grateful to Prof. K. S. Kim of the University of Illinois for his constructive comments on the report by Yang and Freund (1984).

REFERENCES

- Bogy, D. B., 1971, "Two edge bonded elastic wedges of different materials and wedge angles under surface tractions", *Journal of Applied Mechanics*, Vol. 38, pp. 377-386.
- Erdogan, F., Gupta, G. D. and Cook, T. S., 1973, "Numerical solution of singular integral equations", in *Methods of Analysis and Solutions of Crack Problems*, edited by G. C. Sih, Noordhoff, Leyden, pp. 368-425.
- Hu, S. M., 1979, "Film-edge-induced stress in substrates", *Journal of Applied Physics*, Vol. 7, pp. 4661-4666.
- Gradshteyn, I. S. and Ryzhik, I. M., 1965, *Table of Integrals, Series and Product*, Academic Press, p. 36.
- Koiter, W. J., 1955, "On the diffusion of load from a stiffener into a sheet", *Quarterly Journal of Mechanics and Applied Mathematics*, Vol. 8, pp. 164-178.
- Muskhelishvili, 1953, *Singular Integral Equations*, translated by J. R. M. Radok, Noordhoff, Leyden.
- Ramirez, J. C., McNally, P. J., Cooper, L. S., Rosenberg, J. J., Freund, L. B. and Jackson, T. N., 1987, "Development and experimental verification study of piezoelectrically induced threshold voltage shifts in GaAs MESFETs", Brown University Report (submitted for publication).

- Rice, J. R., 1968, "A path-independent integral and the approximate analysis of strain concentration by notches and cracks", *Journal of Applied Mechanics*, Vol. 35, pp. 379-386.
- Timoshenko, S. P. and Goodier, J. N., 1970, *Theory of Elasticity*, McGraw-Hill, New York.
- Yang, W. and Freund, L. B., 1984, *Shear stress concentration near the edge of a thin film deposited on a substrate*, Brown University Report.

FIGURE CAPTIONS

- Fig. 1 A schematic diagram of a film-substrate system; (a) the coordinate system and parameters, and (b) film and substrate separated to illustrate the interfacial shear stress $\tau(x)$.
- Fig. 2 Normalized interfacial shear traction versus normalized distance along the interface, where $\kappa = (1 - \nu^2)E_s / (1 - \nu_s^2)E$, σ_o is the stress in the layer due to mismatch strain, and h is the film thickness.
- Fig. 3 The contour C in the physical plane used for application of the conservation integral (2.19) to obtain the asymptotic form (2.18).
- Fig. 4 A schematic diagram of a periodic array of film segments each of width $2b$ attached to a substrate with spacing $2a$, with each segment subjected to the same mismatch strain.
- Fig. 5 Normalized interfacial shear stress versus distance from the left edge of a film segment, for the configuration shown in Fig. 4, with $a/b \rightarrow \infty$.
- Fig. 6 Normalized interfacial shear stress versus distance from the left edge of a film segment, for the configuration shown in Fig. 4, for several values of the dimensional parameters $\kappa b/h$ and a/b .
- Fig. 7 The normalized strength of the edge stress intensity factor k as defined in (3.8) versus normalized film width for several values of the spacing parameter a/b .
- Fig. 8 Normalized mean normal stress $(\sigma_{xx} + \sigma_{yy} + \sigma_{zz})/3\sigma_o$ versus position (x, z) in the substrate for $\kappa b/h = 10$, $a/b = 1/2$. Half of a film segment covers $0 < \kappa x/h < 10$, $\kappa z/h = 0$ and the interval $10 < \kappa x/h < 15$, $\kappa z/h = 0$ corresponds to half of a gap between segments.
- Fig. 9 Resolved shear stress on planes inclined to the interface at $\pm 45^\circ$ (and normal to the x, z -plane) versus position (x, z) in the substrate for the same parameters as

in Fig. 8. The resolved shear stress is normalized by σ_o .

Fig. 10 Schematic diagram showing straight glide dislocations on the planes inclined at $\pm 45^\circ$ to the interface that relieve the edge stress concentration.

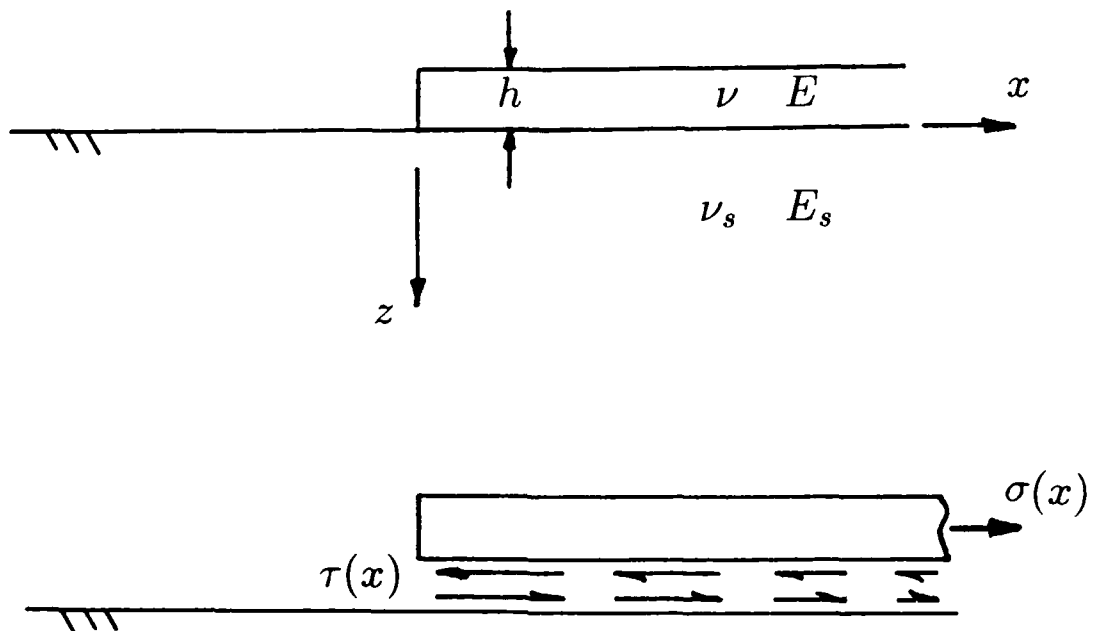
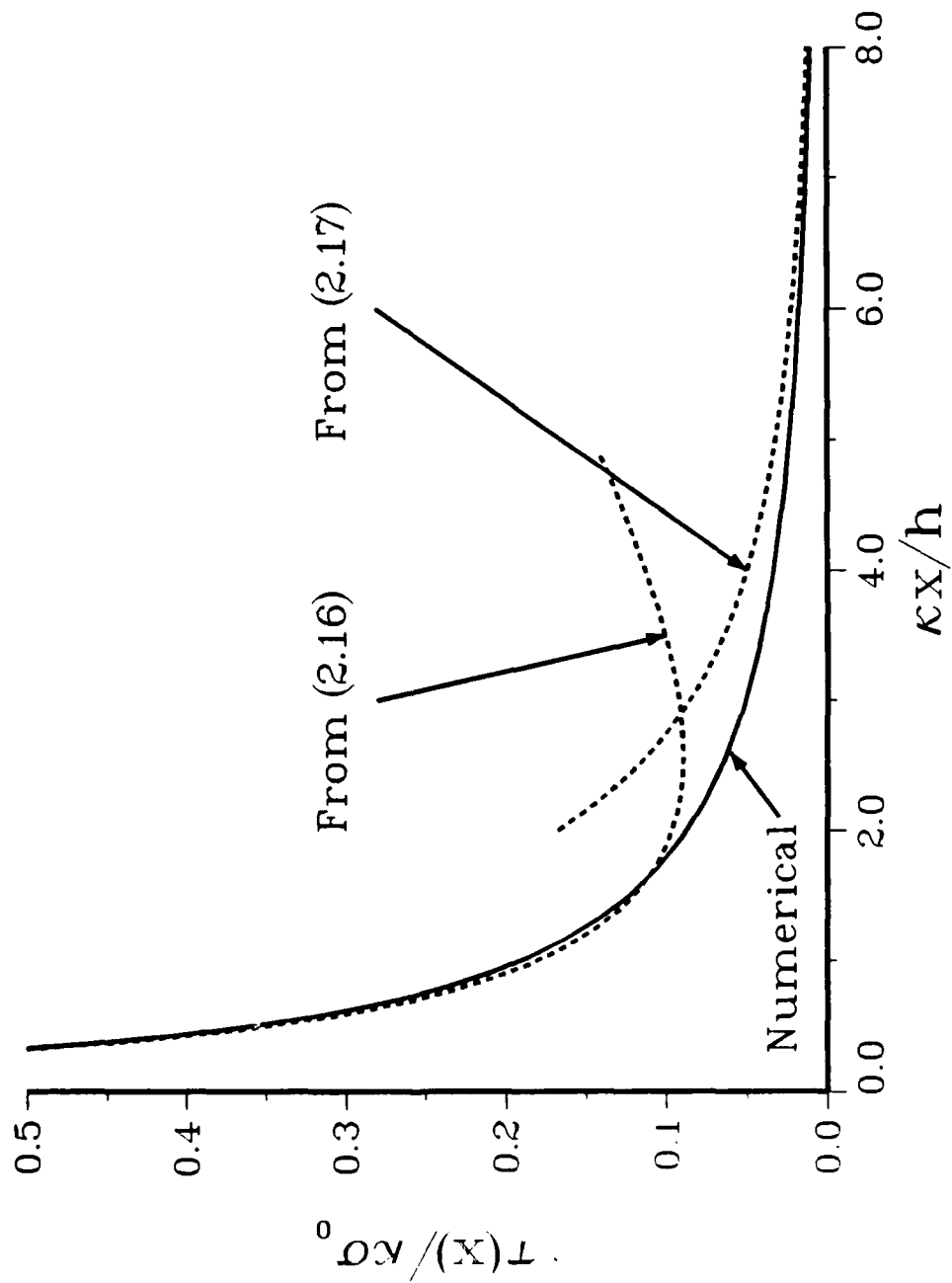


Figure 1

Figure 2



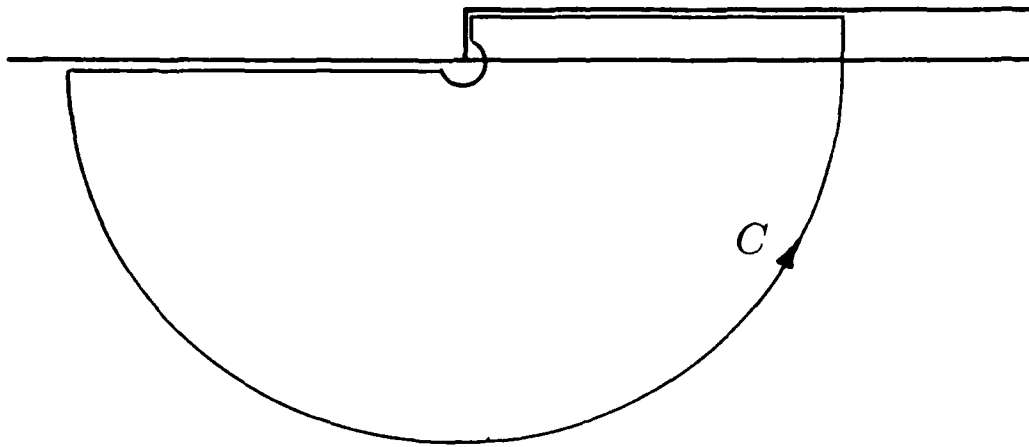


Figure 3

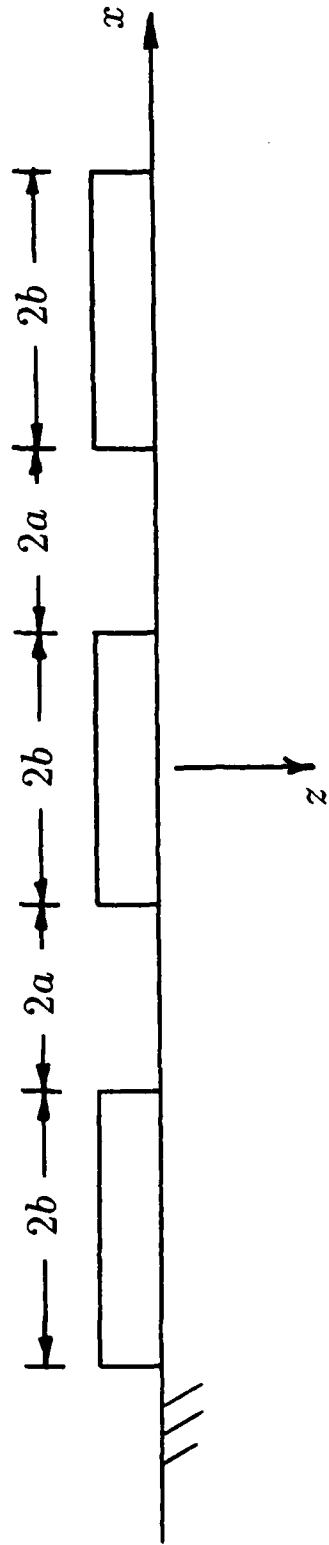


Figure 4



Figure 5

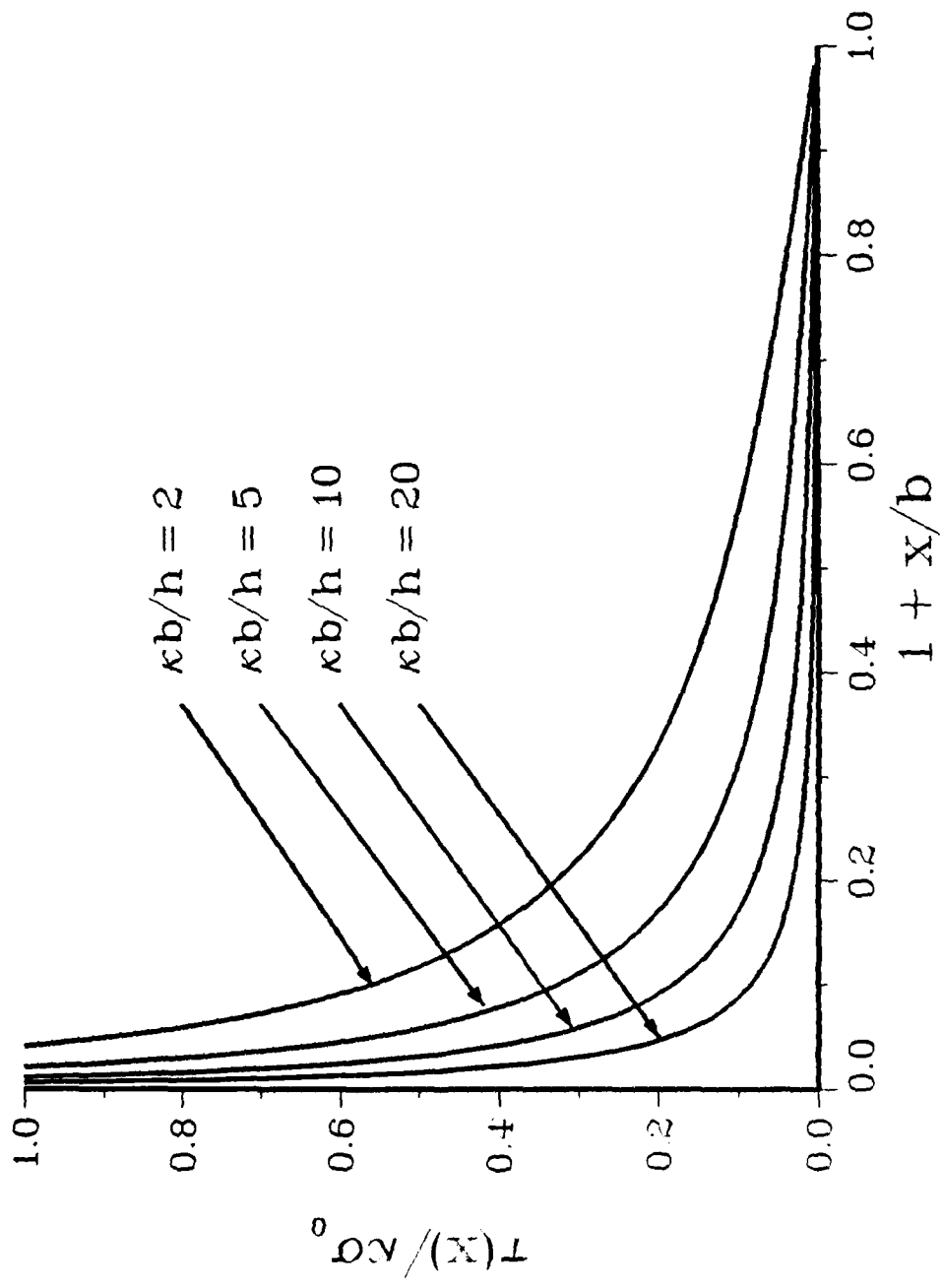


Figure 6

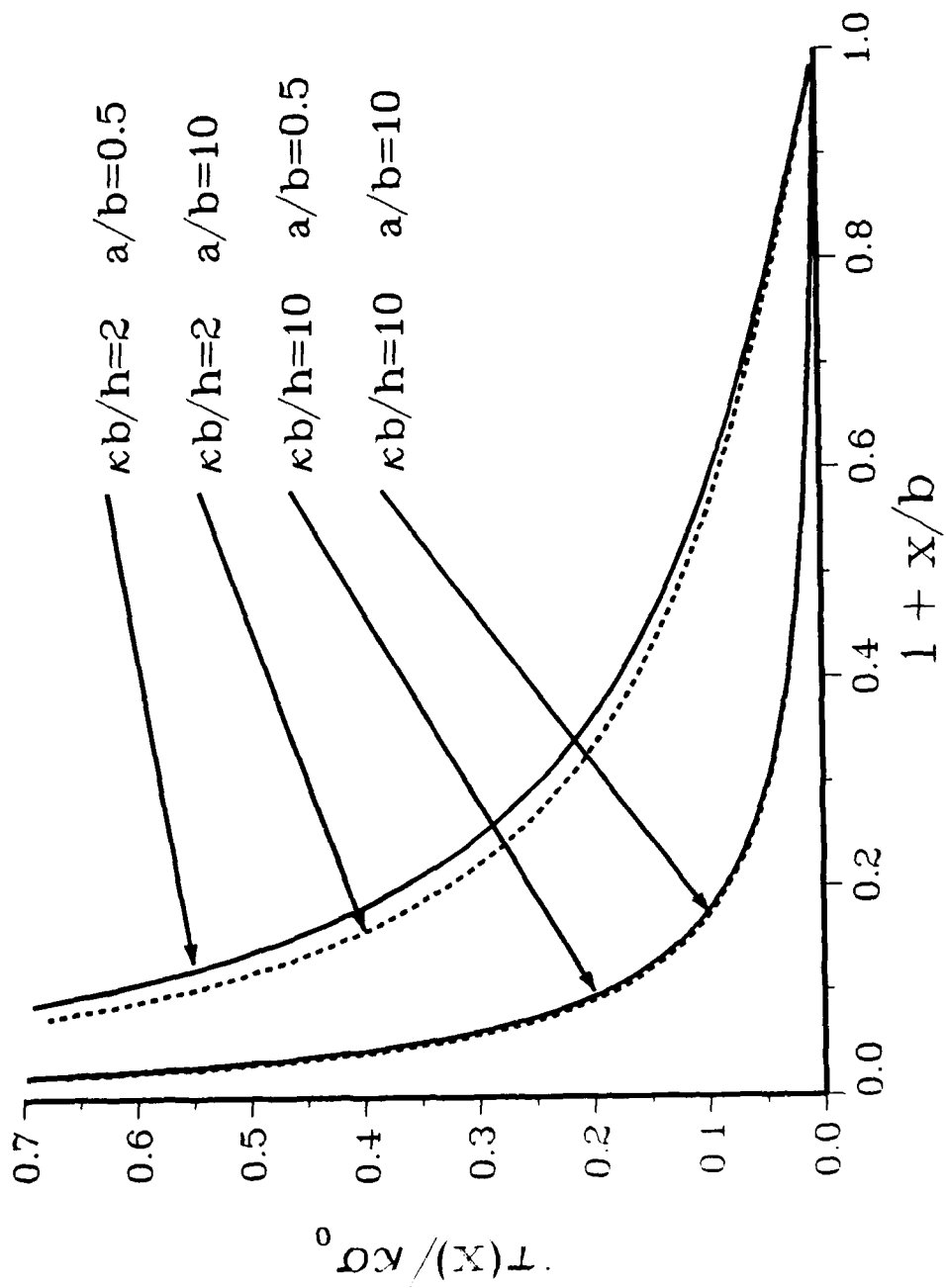


Figure 7

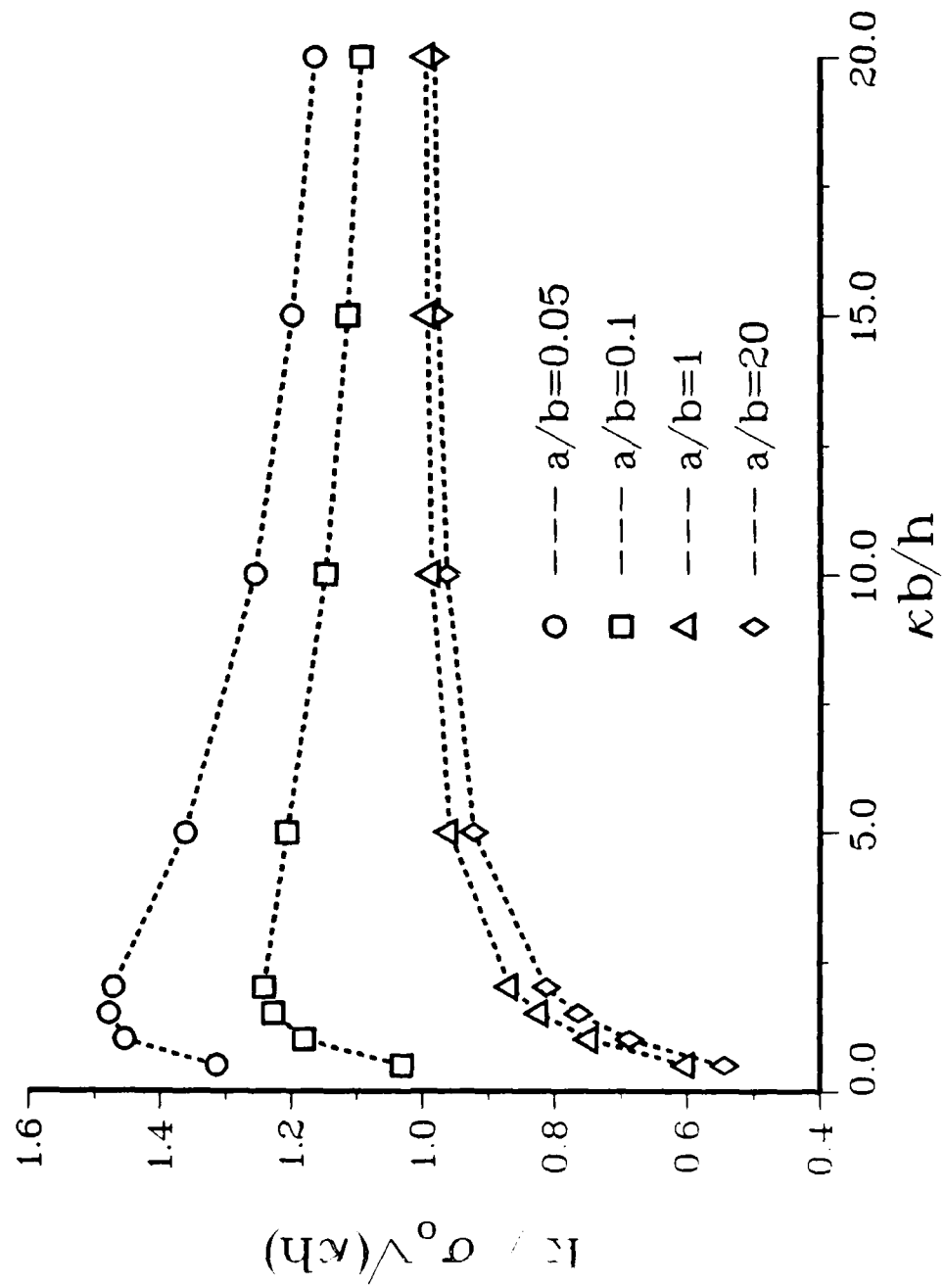


Figure 8

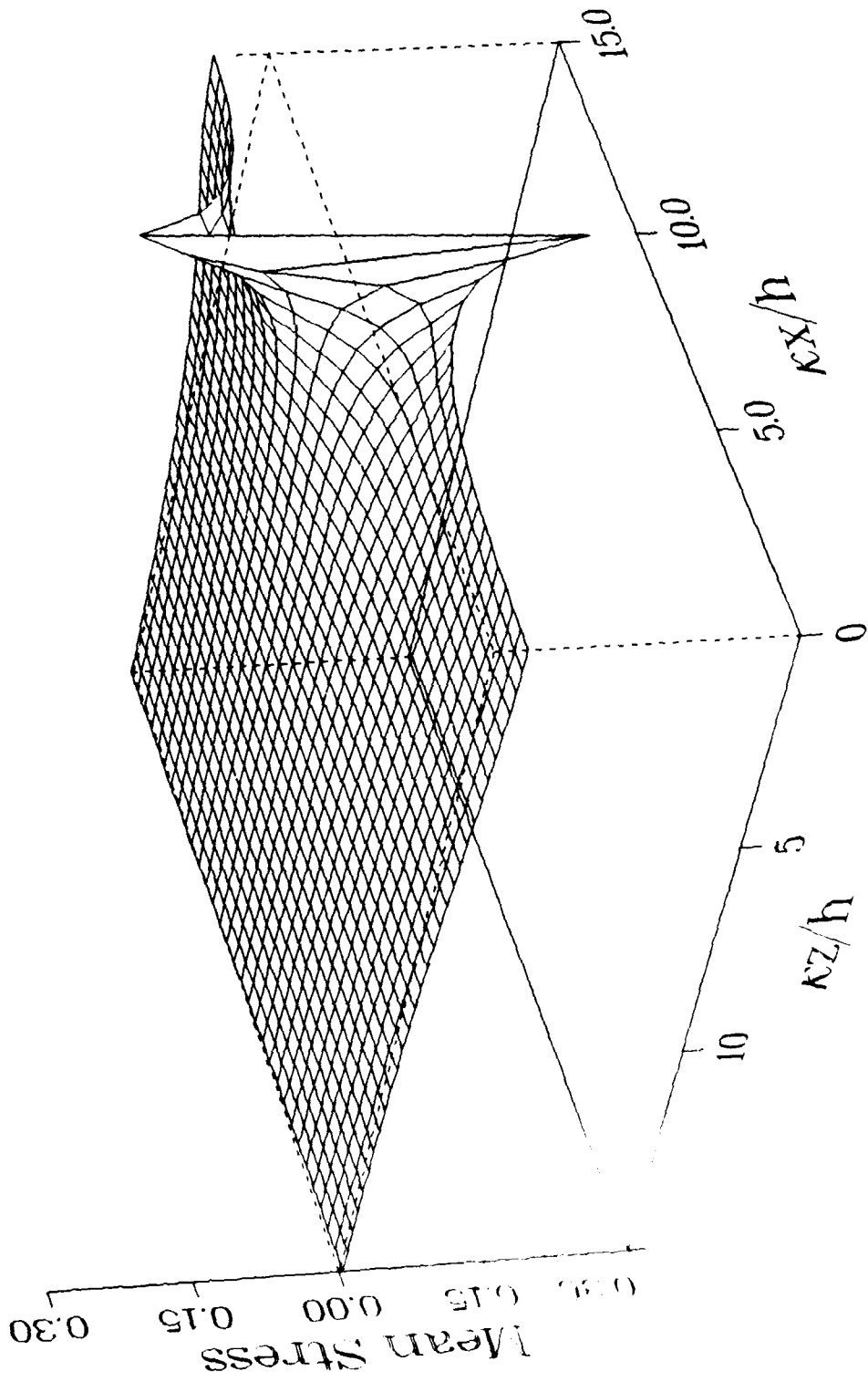
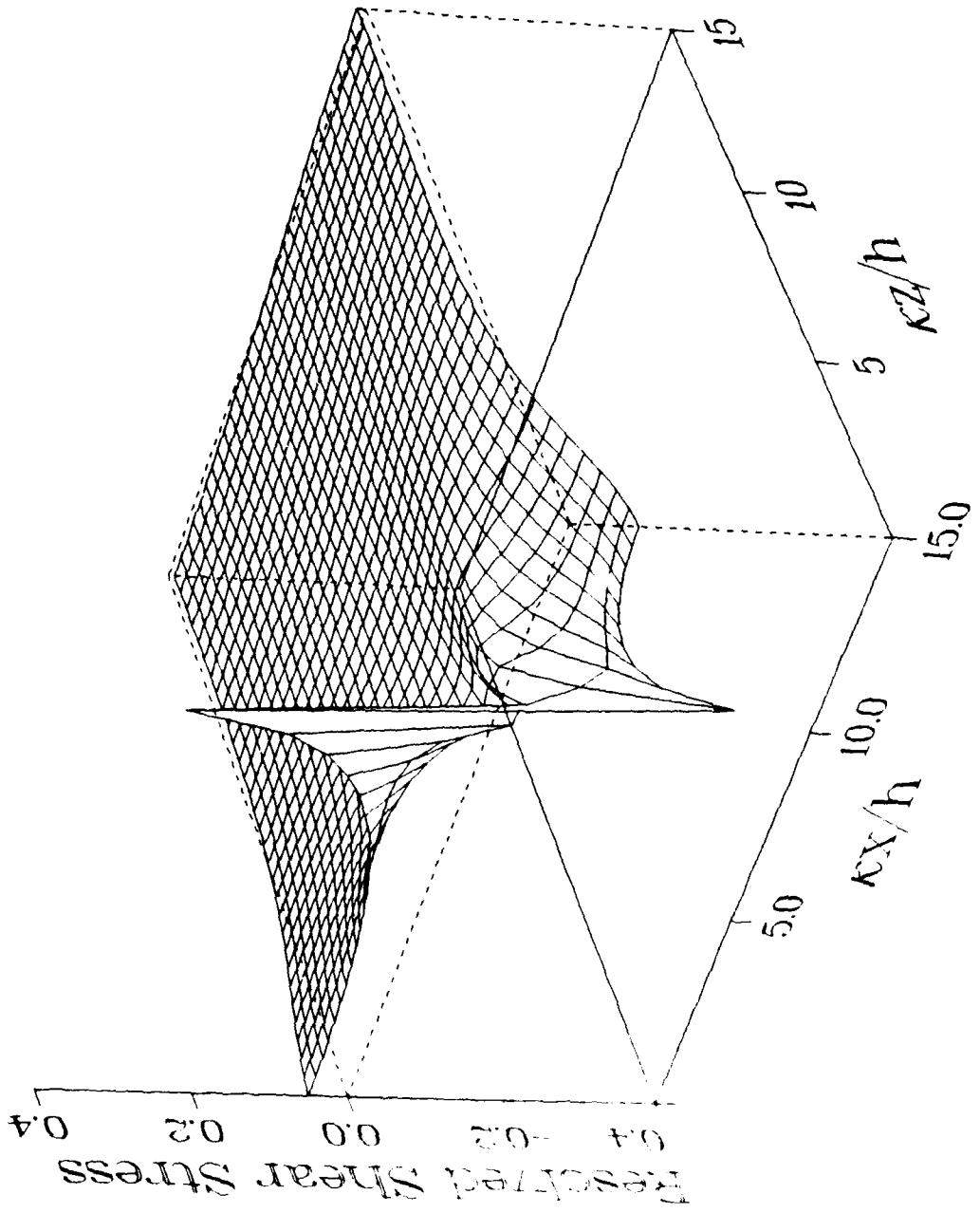


Figure 9



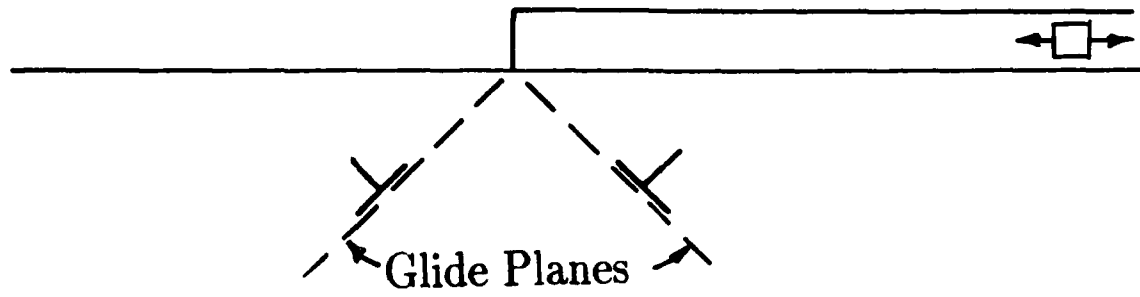


Figure 10

END

DATE

FILMED

DTIC

JULY 88